Photopolymerization Behavior and Phase Separation Effects in Novel Polymer Dispersed Liquid Crystal Mixture Based on Urethane Trimethacrylate Monomer

Nahid Hosein Nataj,[1] Ali Jannesari,[2] Ezeddin Mohajerani,[1] Farhood Najafi,[2] Hossein Jashnsaz[1]

[1]*Laser and Plasma Research Institute, Shahid Beheshti University, Evin, Tehran, Iran*
[2]*Institute for Color Science and Technology (ICST), Tehran, Iran*

Received 13 November 2011; accepted 10 February 2012
DOI 10.1002/app.37000
Published online in Wiley Online Library (wileyonlinelibrary.com).

ABSTRACT: Polymer dispersed liquid crystals (PDLCs) are often formed by polymer induced phase separation, based on photopolymerization of multifunctional acrylate monomers. The emerged morphology is controlled by the interplay between polymerization rate and phase separation dynamics, which depends on different parameters such as monomer structure and functionality. In this work, a new PDLC formulation containing urethane trimethacrylate (UTMA) monomer is introduced, which has different molecular weight evolution, polymer gel point, and polymerization kinetics in comparison with some common ester acrylate (such as TMPTA and DPHPA) based PDLC compositions. UTMA is synthesized and characterized by Fourier transform infrared, ^{1}H-NMR, and ^{13}C-NMR spectroscopic techniques. Simultaneous examination of polymer evolution and LC phase separation by real-time infrared spectroscopy shows that the UTMA based PDLC, which contains trifunctional urethane acrylate monomer, has greater amount of bond conversion, polymerization rate, and liquid crystal (LC) phase separation in comparison with TMPTA based PDLC. In spite of the acrylate monomers, which show gel point conversions as low as 1.83–5.72%, UTMA reaches to its maximum rate at 19.5% conversion, which causes higher phase separation and therefore greater LC domain size. The experimental results are explained more precisely by means of SEM and optical microscopy analyses. The results are confirmed by electro-optics measurements. © 2012 Wiley Periodicals, Inc. J Appl Polym Sci 000: 000–000, 2012

Key words: photopolymerization; phase separation; polymer dispersed liquid crystal; real time infrared spectroscopy; electro-optical properties

INTRODUCTION

Polymer dispersed liquid crystal (PDLC) composites have a wide range of applications, such as flexible displays, tunable lenses, and optical switches.[1–5] The formation of PDLCs is typically induced by photopolymerization.[6,7] A typical photocurable PDLC contains liquid crystal (LC), monomer and initiator. It is known that during photopolymerization of monomer, the LC loses solubility in the polymer and separates into a distinct phase through either liquid-liquid or liquid-gel demixing.[6] Upon phase separation, PDLCs take one of two morphologies: droplet ("swiss cheese") or interconnected (polymer-ball). The control of the film morphology is very important as it serves to modulate the electro-optical properties of PDLC films. Much work has been done to optimize the switching properties, to get a high contrast at a low switching voltage, high switching speed, and low hysteresis.[7–9] The emerged morphology is controlled by the interplay between polymerization rate and phase separation dynamics, which depends on different parameters such as LC concentrations, irradiation intensity, exposure time, reaction temperature, and polymer composition. In any case, the mixture composition plays the most important role in determining the morphology of the recorded structures and their final optical and electro-optical properties such as switching voltage and transmittance.

The formation of PDLCs through photopolymerization has been widely investigated in acrylate and thiol-ene systems.[10–14] In acrylate systems, mixture compositions contain acrylate monomers with various chemical structures and functionality. The polymerization behavior of acrylate monomer in creating polymer with gel point conversion, as low as 3%, causes LC demixing in PDLC systems to predominately occur through liquid- gel demixing.[6] The kinetics of acrylate polymerization dictates the morphology of a given PDLC. The variation of polymerization rate affect on the size of the LC domains and the size of the phase separated polymer areas. The electro-optical behavior of acrylate-based PDLCs is not optimal, as the anchoring of the LC to the polymer is quite strong. Ultimately, the significant anchoring energy in acrylate based PDLCs results in

Correspondence to: E. Mohajerani (e-mohajerani@sbu.ac.ir).

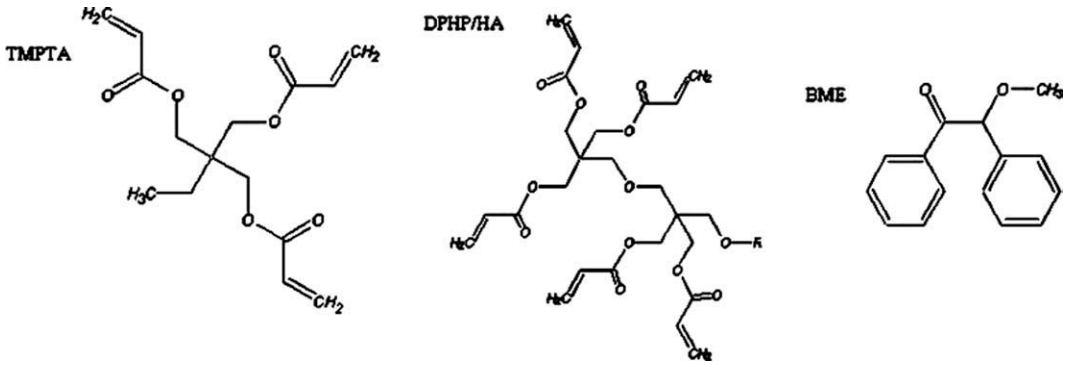

Figure 1 Chemical structures of the components of the PDLC mixtures.

high fields being necessary to switch PDLC scattering. However, the gel point in thiol-ene polymers range from 33 to 86% as calculated from the well-known gel point equation. With such high gel point conversion, LC phase separation in thiol-ene based PDLCs predominantly occurs via liquid-liquid demixing. As shown in examinations of nematic fraction in thiol-ene based PDLCs, liquid-liquid demixing occurs at a faster rate than liquid-gel demixing leading to increased nematic fraction in PDLCs with high gel point conversion.[15–17]

In this study, we introduce a new multifunctional acrylate monomer; urethane trimethacrylate (UTMA) based PDLC, which shows different polymerization behavior, LC phase separation and electro-optical performance in comparison with some common ester acrylate based PDLC compositions such as TMPTA and DPHPA. Four samples containing urethane and ester acrylate monomers are prepared. The photopolymerization behavior of PDLC compositions is studied simultaneously with direct examination of LC phase separation by real-time infrared spectroscopy (RTIR). The understanding gained through RTIR examination of polymerization behavior and LC phase separation is confirmed by optical microscopy and scanning electron microscopy (SEM) imaging of PDLC morphology. Ultimately, the electro-optic switching behavior of the fabricated PDLC films is compared.

EXPERIMENTAL

Materials and sample preparation

Materials

The multifunctional acrylate monomers used are trimethylolpropane triacrylate (TMPTA) and di-pentaerythritol penta/hexa acrylate (DPHPA) from Aldrich. All PDLC formulations contain Benzoin Methyl Ether (BME), also from Aldrich, as UV photoinitiator. The molecular structure of the components is shown in Figure 1.

Materials used for synthesizing UTMA are 1,8-diamino-4-aminomethyloctane (Chemos GmbH, Germany), dichloromethane (CH_2Cl_2), triethyl amine (TEA), trichloromethyl chloroformate, dibutyltin dilaurate (DBTDL), and hydroxyethyl methacrylate (HEMA), as received from Merck without further purification.

Synthesize and characterization of UTMA

A solution of 1,8-diamino-4-aminomethyloctane (17.33 g; 0.1 mol) and TEA (60.6 g; 0.6 mol) in CH_2Cl_2 (100 mL) was added drop wise to a stirred solution of trichloromethyl chloroformate (35.61 g; 0.18 mol) in CH_2Cl_2 (100 mL) at 0°C over a period of 30 min. The ice bath was then removed and the solution stirred for a further 60 min in 40°C before evaporation of the volatiles *in vacuo*. Triethyl ammonium chloride filtered from organic phase. The solvent was removed *in vacuo* to yield 1,8-diisocyanato-4-(isocyanatomethyl)octane as liquid (23.1 g; 92%).[18] Then, UTMA was synthesized by reaction of 1,8-diisocyanato-4-(isocyanatomethyl)octane (12.5 g; 0.05 mol) and HEMA (23.4 g; 0.18 mol) in presence of DBTDL (0.03 g) as catalyst. Figure 2 shows the synthesis of UTMA schematically.

The structure of UTMA is confirmed by the ^{1}H-NMR, ^{13}C-NMR, and Fourier transforms infrared (FTIR) spectral data. The protons of UTMA on ^{1}H-NMR spectrum are CH_3 of HEMA in 1.9 ppm, unsaturated CH_2 of HEMA in 5.5 and 6 ppm, OCH_2 HEMA in 4.2 and 4.3 ppm, CH_2—NHCO in 3 and 3.1 ppm, and central CH_2 and CH of UTMA are in 1.3, 1.4, and 1.5 ppm. NH urethane band is in 5.1 ppm as a broad peak. The carbons of UTMA on ^{13}C-NMR spectrum are CH_3 of HEMA in 18.6 ppm, unsaturated CH_2 and C of HEMA in 126.3 and 136.4 ppm, carbonyl group of HEMA in 168 ppm, carbonyl group of urethane band in 156 ppm, OCH_2 of HEMA in 61.2 and 66.6 ppm, CH_2—NHCO in 41.2 and 43.1 ppm, and central CH_2 and CH of UTMA are in 26.5, 26.6, 27.9, and 30 ppm.

The FTIR spectrum of UTMA shows stretching band of N—H urethane in 3380.98 cm^{-1}, stretching

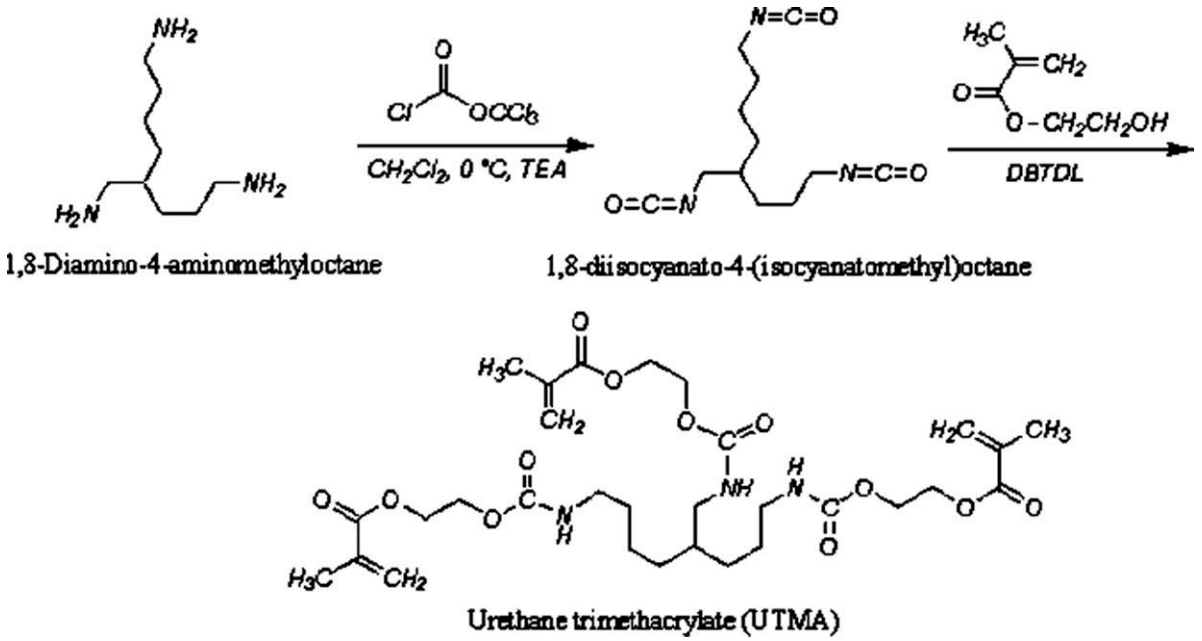

Figure 2 Synthesis of UTMA.

band of C—H aliphatic unsaturated in 3105.37 cm^{-1}, stretching band of C—H aliphatic saturated in 2937.44 and 2866.90 cm^{-1}, stretching band carbonyl group of HEMA monomers connect to UTMA in 1695.52 cm^{-1} and stretching band carbonyl group of urethane bands in 1638.32 cm^{-1}.

Sample preparation

We used four different photocurable mixtures in which the monomer composition changes as explained in the following: Pre polymer 1 (PP1) composite contains neat synthesized UTMA while PP2 and PP3 contain TMPTA/DPHPA and neat TMPTA, respectively. The combination of TMPTA and UTMA is named PP4. The content of monomers is shown in Table I. The refractive indices of the photopolymerized composites are experimentally obtained using Abbe refractometer and reported in Table I. In this work E7, from Merck, with optical anisotropy (Δn) 0.225 and ordinary refractive index (n_o) 1.5216 is used as LC. Four samples containing the mixture of PP1 to PP4 and 27 wt % LC are also prepared and named PDLC1 to PDLC4, respectively. All eight samples (PP1-4 and PDLC1-4) contain 3 wt % BME as UV photoinitiator. Ready-made cells (thickness = 7.9 μm) with ITO as transparent electrodes were filled with the mixture by means of the capillary action.

Double bond equivalent weight (DBEW)

To characterize the multifunctional acrylate monomers based on their both molecular weight and monomer functionality, as two effective parameters in polymerization kinetics and hence the phase separation of the PDLC compounds, DBEW is introduced. DBEW is defined as $\overline{M}/\overline{f}$, in which $\overline{M}$ is average molecular weight of monomer composition and $\overline{f}$ is average functionality of monomer composition. DBEW of PP1, 2, 3, and 4 are calculated and reported in Table I. The amount of DBEW for UTMA is about twice that of TMPTA and TMPTA/DPHPA.

Measurement of T_g

For calculating the glass transition temperature (T_g), the prepolymer samples 1–4 are irradiated with a UV lamp for 7 min. Then the T_g of the cured acrylate polymer compositions is measured by using Pyris6 Perkin-Elmer Differential Scanning Calorimeter, DSC

TABLE I
Specifications of the Samples

Sample	Composition	Content (%)	DBEW (g/eq)	Refractive index	T_g (°C)
PP1	UTMA/BME	9 7: 3	204.3	1.537	63.5
PP2	DPHPHA/TMPTA/BME	52 : 45 : 3	101.9	1.519	63.5
PP3	TMPTA/BME	97 : 3	98.7	1.521	64
PP4	UTMA/TMPTA/BME	72 : 25 : 3	159.8	1.516	63

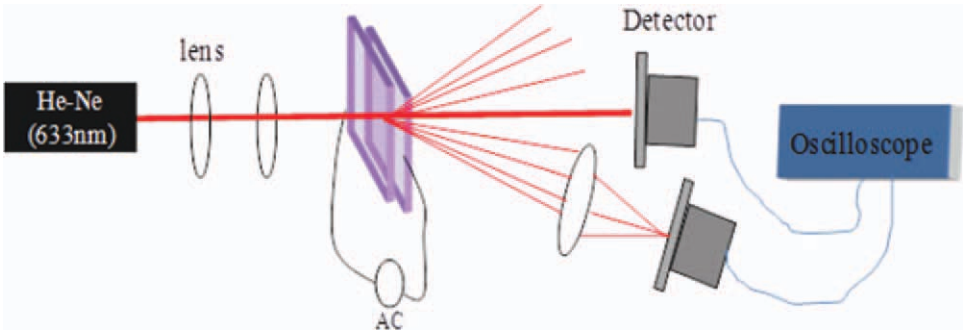

Figure 3 Experimental set up for electro-optics measurement. [Color figure can be viewed in the online issue, which is available at wileyonlinelibrary.com.]

apparatus. A rate of 10°C min^{-1} (heating and cooling) is used in the temperature range −50 to +200°C. The polymer glass transition temperature is determined from the midpoint of the transition range of the thermograms. The values of the calculated T_g of four samples are reported in Table I.

Methods

Real time infrared spectroscopy

A FTIR spectrometer (Perkin-Elmer Spectrum One) equipped with an IR detector was adapted to enable RTIR. Samples are exposed to a UV source lamp (~ 30 mw cm^{-2}). Spectra are collected every 1 s at 4 cm^{-1} resolution during the course of photopolymerization. Subsequently, the reduction in the IR absorbance of the acrylate double bonds at 812 cm^{-1} (C=C stretching) is monitored to calculate the double bond conversion. The conversion of the acrylate functional group at a given time is given by

$$\text{Percent Conversion} = \frac{A_t - A_0}{A_0} \times 100\%$$

where at a specified wave number, A_t is the IR peak height at time t and A_0 is the peak height before polymerization. In addition to examining polymer evolution, RTIR is useful in examining LC phase separation and order in polymer/LC systems.[14,19,20] The absorbance of the cyano moiety in LC s is shown to be mesophase dependent. The extent of the decrease in cyano absorbance in 2225 cm^{-1} from the value before polymerization is indicative of the amount of LC in the nematic phase in the formed PDLC. The thermotropic nature of E7 was utilized to determine the absolute absorbance change of this LC in its isotropic state versus its nematic state. On a unit scale, the absorbance of bulk E7 at 2225 cm^{-1} in the isotropic phase is 1.0 and 0.78 in the nematic phase. Before polymerization of PDLCs, E7 is isotropic as the formulation is homogenously mixed. Upon phase separation, the LC undergoes an isotropic to nematic transition. The ratio of the absorbance change at 2225 cm^{-1} during the polymerization of PDLCs to the absolute absorbance change of the neat LC was used to calculate the fraction of LC in the nematic phase (nematic fraction):

$$\text{Nematic fraction} = \frac{A_0 - A_t}{0.22}$$

where A_0 is the average absorbance at 2225 cm^{-1} at the beginning of the polymerization and A_t is the absorbance at time t during the polymerization.

Morphology

A scanning electron microscope (SEM, LEO1455 VP, and 10 kV) is used to examine directly polymer/LC morphology. The LC of PDLC samples is first extracted using methanol (MeOH). The samples are soaked in MeOH for several hours and then dried under vacuum. For optical microscopy, the mpl-15 BEL microscope is used with various lens magnifications ranging from 50× to 600×.

Electro optics measurement

The experimental set up for electro-optic measurement is shown in Figure 3. The transmission of He—Ne laser (633 nm and 3 mw) through the PDLCs is examined with a photodetector as voltage is increased stepwise (square wave, 1 kHz).

RESULTS

RTIR spectroscopy

RTIR is a well-known technique for studying the influence of the monomer characteristics on morphology and electro-optic response of PDLCs. RTIR spectroscopy directly measures conversion and has been a useful tool to independently monitor the conversion of distinct functional groups.[6,21] Figure 4 illustrates IR spectra of UTMA monomer (PP1)

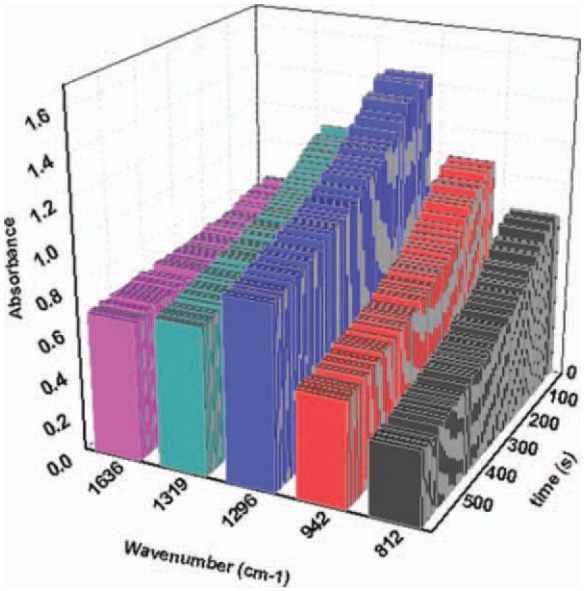

Figure 4 RTIR spectra of UTMA (PP1) irradiated for 10 min with UV lamp (~ 30 mw/cm^2). [Color figure can be viewed in the online issue, which is available at wileyonlinelibrary.com.]

collected by RTIR, subjected to irradiation at room temperature for 10 min using the UV lamp. The change in the peaks area at 812 cm^{-1}, which corresponds to the stretching of the acrylate double bonds, is monitored for the conversion evaluation.

Figure 5(a) shows RTIR evaluation of C=C double bond conversion versus time for the samples PP1 to PP4. Initial portion of the curves involves a rapid increase in double bond conversion due to the increase in the polymerization rate and then, levels off when the conversion reaches its maximum value. It depicts that as Equivalent weight of double bond (DBEW) in monomer composition decreases, double bond conversion decreases from nearly 56% in UTMA to ~ 22% in TMPTA. Although the amount of bond conversion for the mixture of DPHPA/TMPTA after 10 min UV irradiation is greater slightly, the evolution of double bond conversion with time for the pure TMPTA and mixture of DPHPA/TMPTA (with the similar DBEW values) is nearly identical. It also shows that the combination of UTMA/TMPTA has the least bond conversion evolution. Figure 5(b) presents the curves of bond conversion of PP1, which contains UTMA, and its mixture with 27% LC E7 (PDLC1). As seen, the amount of overall double bond conversion is reduced in the presence of LC.

In general, polymerization of multifunctional acrylate monomers forms crosslinked networks of infinite molecular weight (i.e., gelled polymer) at conversion as low as 2–5%. Monomer mobility in the polymer network is extremely limited due to the constraints of the highly crosslinked, gelled polymer. In PDLC polymerization, the LC acts as a plasticizer that reduces diffusional constraints and subsequently enables greater monomer mobility, while providing more accessible space for the polymerization of acrylate to occur. However, once phase separation occurs, some unreacted monomers could be trapped within the LC-rich region and thus the probability of collision between the growing polymers and the residual monomers is diminished, resulting in decreased overall double bond conversion.[21]

To understand whether LC contributes to the polymerization behavior of acrylate monomers, the bulk (just monomer compositions; PP1–PP4 samples) and PDLCs (i.e., monomers compositions with 27%

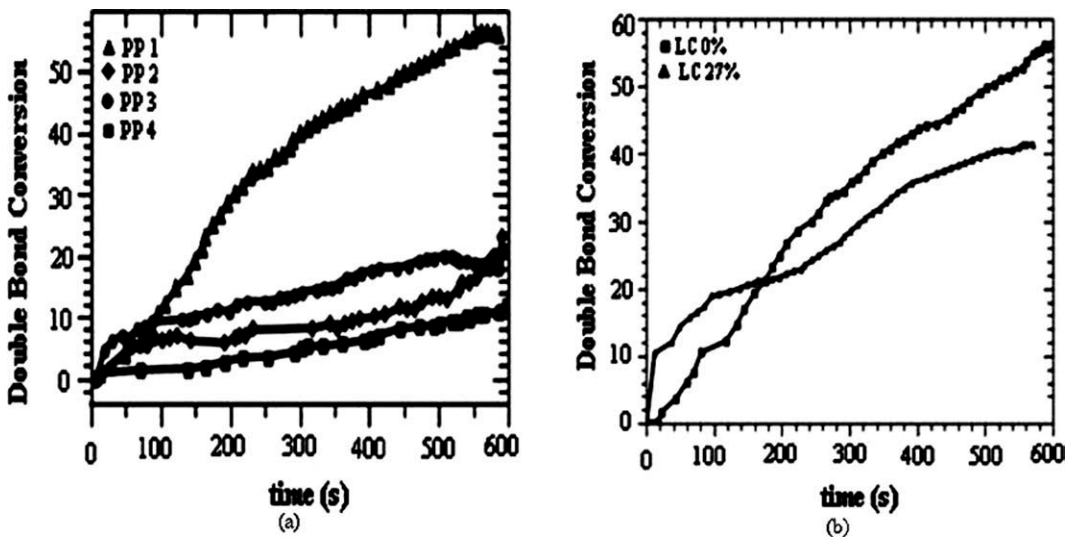

Figure 5 (a) RTIR spectra of samples PP1–PP4 during 10 min UV irradiation. (b) The influence of adding 27% LC on photopolymerization of UTMA (PP1) under 10 min UV irradiation.

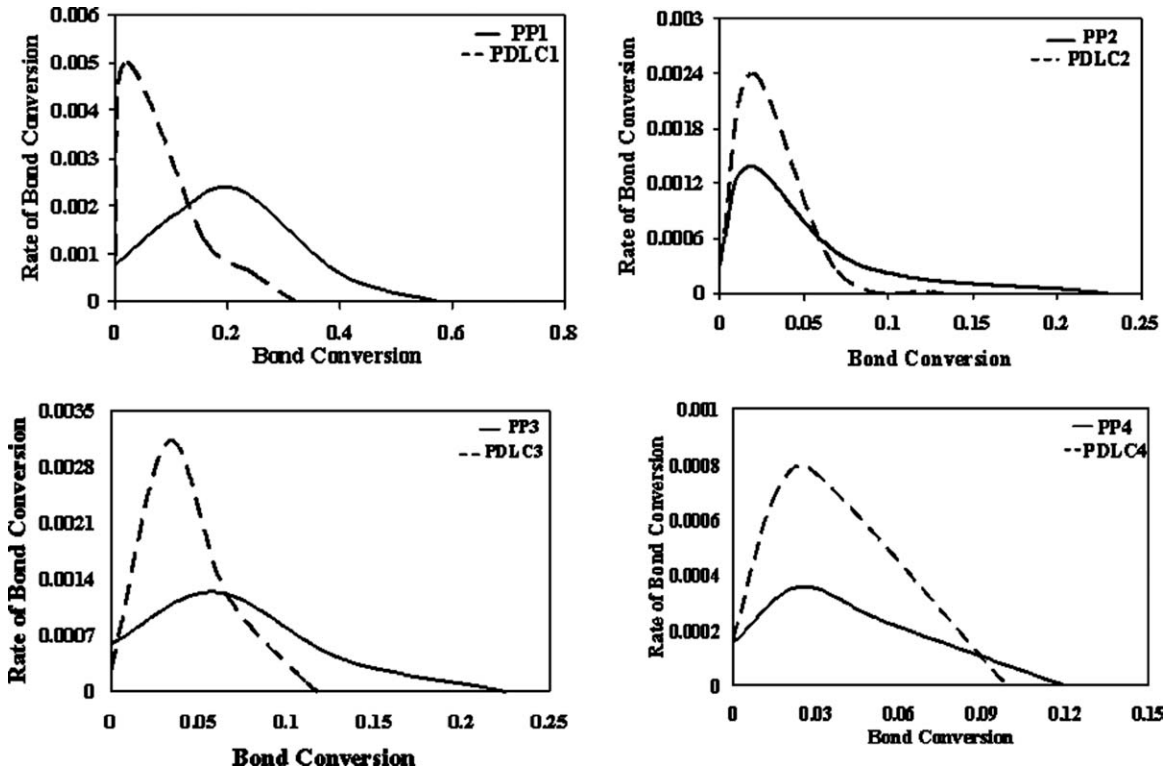

Figure 6 Rate of conversion vs double bond conversion for PP1 to PP4 and corresponding PDLC1 to PDLC4 samples.

E7; PDLC1–PDLC4) polymerization rates ($d\alpha/dt$), during 10 min irradiation of UV lamp, are plotted versus conversion. As shown in Figure 6 in all samples, an increase of polymerization rate is observed up to a maximum and then, the polymerization rate falls to almost zero even though an appreciable amount of unreacted monomers exists in the polymerizing mixture. Interestingly, in all four monomer compositions, adding LC increases the polymerization rate due to LC plasticizing effect, which enables greater monomer mobility. However, in our PDLC samples, the overall bond conversion is decreased in comparison with the corresponding monomer compositions PP1–PP4, which could be related to the unreacted trapped monomers within the LC domains during the phase separation.[21] The maximum polymerization rate of the monomer compositions and corresponding limiting conversions are 0.0024 s^{-1}-57% for PP1, 0.00138 s^{-1}-23% for PP2, 0.00124 s^{-1}-22% for PP3, and 0.000356 s^{-1}-12% for PP4 samples, respectively. For PDLCs, the maximum polymerization rate of the monomer compositions and limiting conversions are 0.005 s^{-1}-32% for PDLC1, 0.0024 s^{-1}-13% for PDLC2, 0.0031 s^{-1}-12% for PDLC3, and 0.0008 s^{-1}-10% for PDLC4 samples, respectively. It is well known that in photopolymerization of multifunctional monomers, overall conversion reaches to lower than 100%. This behavior relates to typical bulk free radical polymerization run, at temperatures lower than the glass transition temperature of the polymer. It is also notable that for PP1–PP4, the polymerization rate of the UTMA based PP1 is significantly greater than that of other compositions. It is 57.5 and 51.7% greater than the polymerization rates of TMPTA (PP3) and DPHPA/TMPTA (PP2) compositions, respectively. For PP4/PDLC4, which contains both TMPTA and UTMA, it seems that the low polymerization rate and bond conversion is dependent to the limiting effect of TMPTA (with microgelation as low as 3–5%) in the vicinity of UTMA. The analysis of this behavior needs more investigation and in the future works we study it more precisely.

It is known that polymerization of multifunctional acrylate monomers form crosslinked networks of infinite molecular weight (i.e., gelled polymer) at conversions as low as 2%. It is important to note that in UTMA based PP1 composition, the conversion in which crosslinked network is formed (gel point conversion) is 19.5%. The gel point conversion for PP2, PP3, and PP4 is 1.83, 5.72, and 2.56%, respectively.

DBEW of samples is influential on the rate of polymerization and overall bond conversion. As explained before, by increasing the DBEW from TMPTA (PP3) to UTMA (PP1), the rate of polymerization of acrylate monomer is increased. By decreasing the DBEW of monomer composition, the diffusional constraints associated with increased crosslink density reduce monomer mobility, thereby reducing polymerization rate. The DBEW of PP2 and

PP3 is nearly the same. However, the polymerization rate of the mixture of DPHPA/TMPTA, with higher average functionality is greater than that of pure TMPTA. It is also evident that as monomer functionality decreases, the gel point bond conversion decreases from 5.72% in the DPHPA/TMPTA composition (PP2) to 1.83% in TMPTA (PP3).

In addition to influencing polymerization rate and limiting bond conversion, increasing acrylate monomer functionality (or reducing its DBEW) can change the polymer gel point, and the onset of vitrification (i.e., T_g) in PDLCs. In comparison with TMPTA and DPHPA, the length of the molecular spacer between the acrylic moieties in UTMA is greater and the crosslinked bridges in its network are longer. Therefore, the rigidity of the network of UTMA reduces; the vitrification (gelation) occurs at higher degrees of conversion and the limiting conversion increases. As shown in Table I, the measured T_g of cured samples PP1 to PP4 under the UV lamp exposure is similar (about 63°C), which means that the T_g of the completed network of all samples is higher than 63°C and photopolymerization run in all of them has been ceased due to the vitrification occurring around this temperature. Therefore, it seems that the glass transition temperature during the evolution of crosslinking reaction in the UTMA composition (PP1) has elevated slower than that of other compositions. Consequently, the slow rising of T_g during photopolymerization of PP1 sample caused its limiting conversion to be high and about 56%. It shows that the accessibility to the double bonds depend on structural features of the monomers, at least in the last steps of the photo polymerization reaction. It can be concluded that reaction diffusion controlled the termination kinetics. Mobility through reaction diffusion becomes easier than other forms of diffusion for radicals due to the highly crosslinked structure formed during the polymerization of the multifunctional acrylates.[22,23] Besides, the longer molecular spacers between the acrylic double bonds make their diffusion easy. Therefore, the maximum values of the photo polymerization rate increases for the UTMA monomers. However, in the earlier stage of polymerization for the compositions contain TMPTA and/or DPHPA monomers, the branches are generated in the growing macro-radical, limiting its translational diffusion inside the reactive bulk. Thus, the maximum polymerization rates are reached at low conversions (1.83–5.72%) depending on the monomer structure.

The change in IR peak height at 2225 cm^{-1} is shown in Figure 7 for the photo polymerization of UTMA based PDLC (PDLC1). The decrease in IR peak height at 2225 cm^{-1} is associated with the increasing appearance of the nematic phase as LC phase separates. The nematic fraction of the UTMA

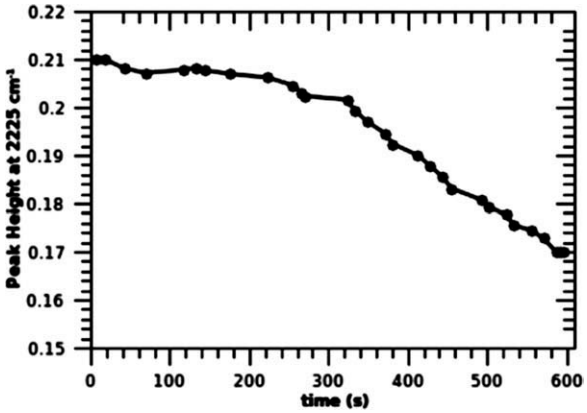

Figure 7 RTIR examination of LC phase separation in polymerization of PDLC1 at 2225 cm^{-1}.

based PDLC (PDLC1) is greater than that of other PDLC composites. The overall nematic fraction of PDLC1 to PDLC4 is 19, 4.5, 14, and 4.5%, respectively.

In general, as monomer functionality increases (decreased DBEW) the nematic fraction is reduced. It is known that regardless of acrylate monomer functionality, LC phase separation begins instantaneously upon photo polymerization. In the immediate stages of photopolymerization, LC phase separation is associated with both liquid-liquid demixing and liquid-gel demixing, as acrylate polymerization is known to form microgels even at very low conversion. As acrylate conversion increases, the evolution of the nematic phase slows at a transition point at which the macrogelation would happen. The double bond conversion, at which this transition occurs, increases with increasing the DBEW of monomer. The onset of macrogelation to 19.5% double bond conversion by increasing the DBEW of monomer in the PDLC1 extends the regime that LC phase separation can occur via liquid-liquid demixing, leading to more overall LC phase separation. This is an interesting behavior of UTMA monomer in comparison with the other multifunctional acrylate monomers, which after 1.83–5.72% conversion reach to their gel point conversion.

To contrast polymer-induced phase separation in PDLCs based on trifunctional acrylate monomers TMPTA and UTMA, the evolution of the nematic fraction (i.e., the fraction of LC molecules in the nematic mesophase) in the samples PDLC1 and PDLC3 is plotted against monomer conversion, as shown in Figure 8. As expected, the appearance of the nematic phase for TMPTA based PDLC (PDLC3) is immediate and steadily increases over the range of double bond conversion until the conversion of about 10% is reached after 10 min UV lamp irradiation. The evolution of the nematic phase is much different for the UTMA based PDLC (PDLC1). Slight increase in nematic fraction is observed until 20%

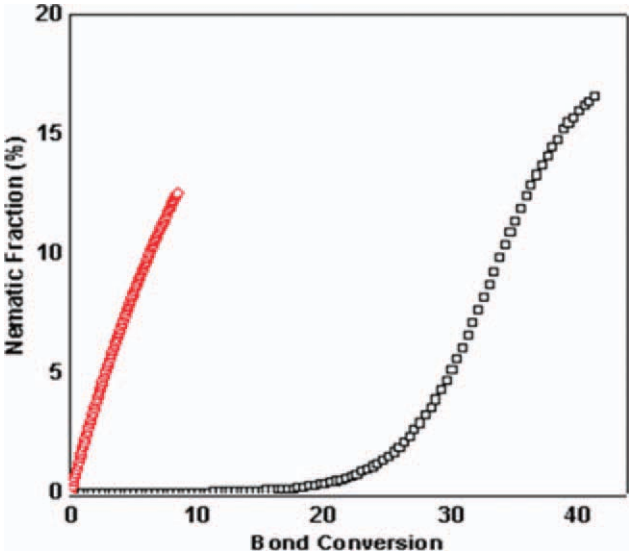

Figure 8 Nematic fraction (%) versus acrylate double bond conversion for UTMA based PDLC (□) and TMPTA based PDLC (◇). [Color figure can be viewed in the online issue, which is available at wileyonlinelibrary.com.]

acrylate bond conversion, followed by a rapid increase that allows 18% of the nematic phase to appear after 10 min curing. About one-fifth of LC phase separation in this PDLC occurs between 30 and 45% conversion. This behavior resembles the thiol-ene based PDLC bond conversion and phase separation.[6]

Previous examination of polymerization induced phase separation in acrylate-based PDLCs has shown that both the onset of gelation and vitrification are influential on the onset and evolutions of LC phase separation. Since the gel point of acrylate PDLC systems is reached almost immediately after polymerization, LC phase separation primarily occurs via liquid-gel demixing; that is, the LC is phase separating from a gelled polymer. Our results reveal that the gel point of UTMA is considerably greater than that of common acrylate monomers such as TMPTA. The increased gel point of UTMA shifts the onset of liquid-gel demixing, increasing the participation of liquid-liquid demixing, and LC phase separation. Subsequently, the LC droplets have more time to grow and coalesce, increasing LC droplet size.

Morphological development

Figure 9 shows the optical micrographs depicting the morphological evolution of four PDLC mixtures.

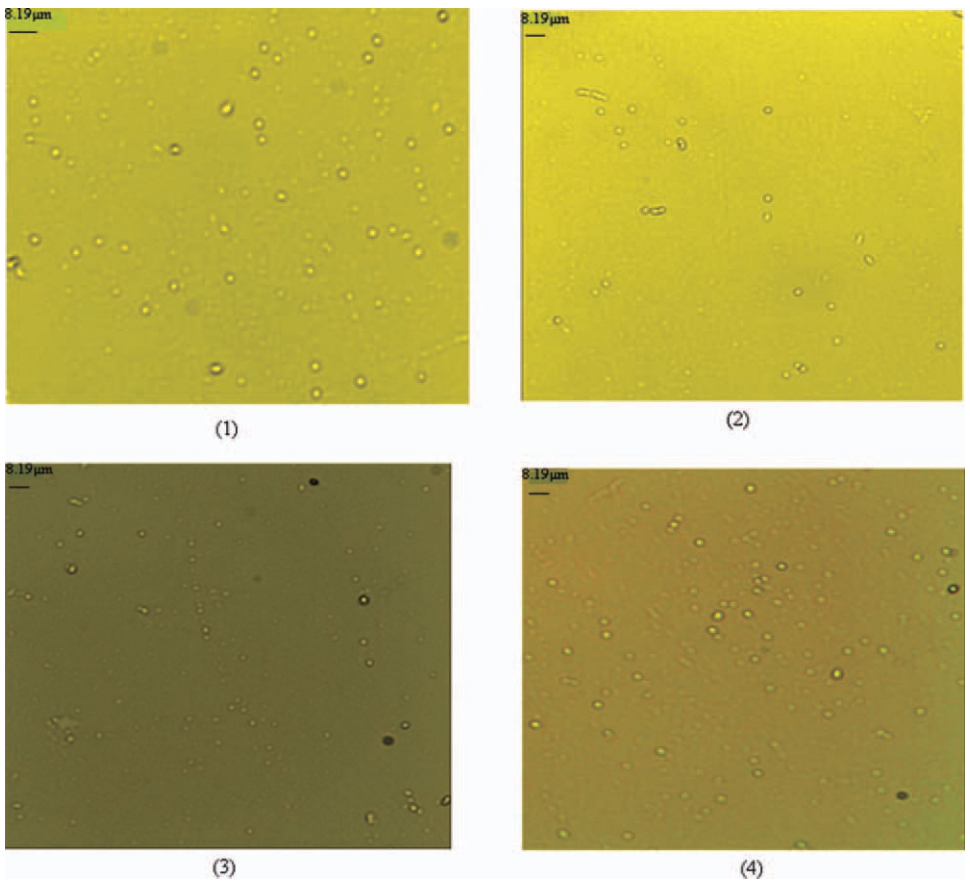

Figure 9 Optical microscopic images of PDLC (1–4) samples after 10 min UV irradiation. [Color figure can be viewed in the online issue, which is available at wileyonlinelibrary.com.]

TABLE II
Electro-Optic Switching Behavior of PDLC Compounds

PDLC	Rise time	Decay time	Average LC droplet size	Switching Field (V/μm)
PDLC1	679 μs	4 ms	950 nm	9.4
PDLC2	84 μs	1 ms	910 nm	13.7
PDLC3	75 μs	340 μs	725 nm	19.4
PDLC4	52 μs	2 ms	890 nm	10.6

As discussed in Section RTIR spectroscopy, the macrogelation in TMPTA based PDLC (PDLC3) occurs faster than that of DPHPA/ TMPTA based PDLC (PDLC2) with higher average monomer functionality. That is why the size of LC domains in PDLC2 is greater than that of PDLC3, as reported in Table II. It is also clear that the size of LC domains in UTMA based PDLC (PDLC1) is greater than that of other PDLC compounds due to its higher bond conversion (for macrogelation and vitrification) and corresponding greater LC phase separation.

The morphology of PDLCs is also characterized with SEM. Since the LC was extracted prior to imaging, the LC domains are indicated by the void spaces (dark areas) present in the polymer morphology. As shown in Figure 10(a–d), the PDLCs possess a polymer ball type morphology, which is common in acrylate based PDLCs.[1] The SEM image of PDLC1 (with DBEW = 204.3 g/eq) shows the greatest average size of the polymer balls and the void spaces (extracted LC) in comparison with the other samples. Comparing the morphology of PDLC2 and PDLC3, with the same DBEW but different functionality, also shows that increasing acrylate monomer functionality reduces the amount of void space (black), indicating less LC phase separation. The comparison of the polymer/LC morphology resulting from the two PDLC formulations with different polymerization behavior: UTMA based PDLC and ester acrylate (TMPTA or TMPTA/DPHPA) based PDLC, highlights how the polymerization behavior dictates the morphology. UTMA based PDLC contains large polymer clusters and large LC domains (dark area), but ester acrylate based PDLCs (samples 2 and 3) shows an integrated polymeric matrix containing small LC domains. PDLC4, which contains both UTMA and TMPTA, shows a combination of the two-mentioned morphology in which polymer cluster are embedded in an integrated matrix.

Electro optics measurements

The sensitivity of our mixtures to an external electric field is investigated by slowly increasing its amplitude at a fixed frequency of 1 kHz, as shown in

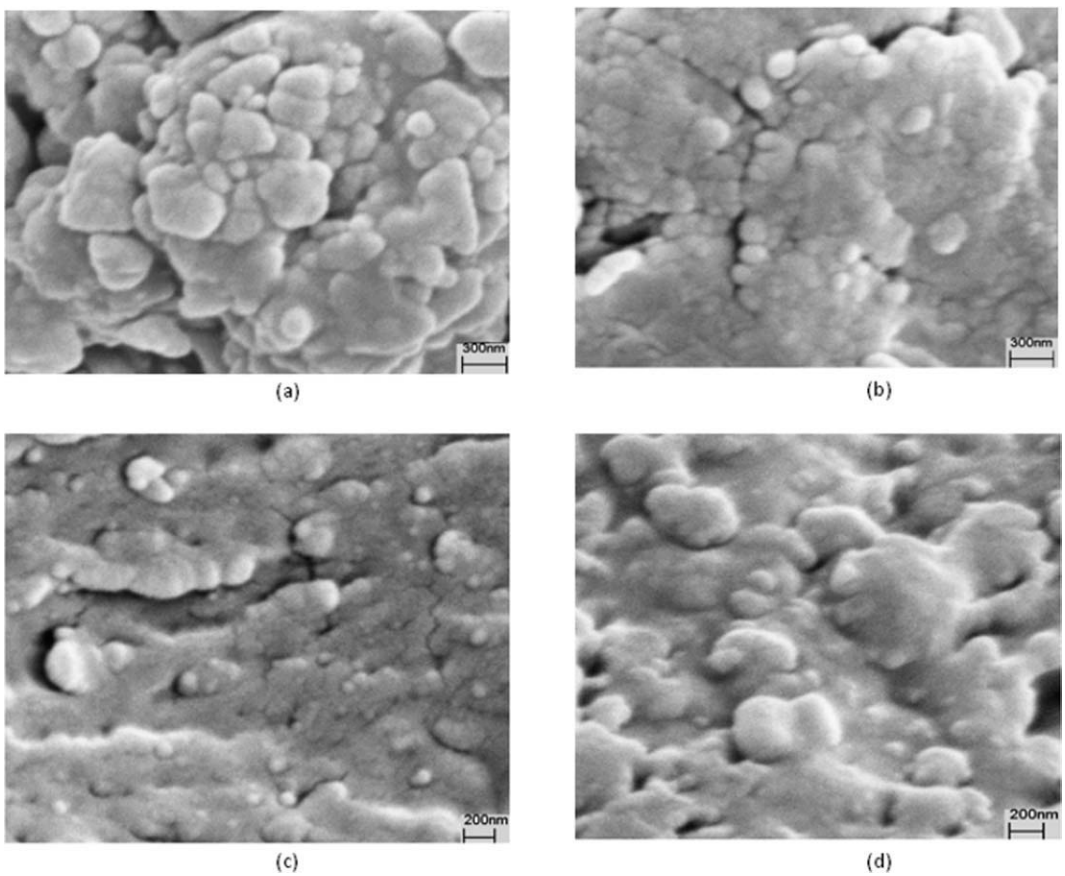

Figure 10 SEM micrographs of PDLC1–PDLC4.

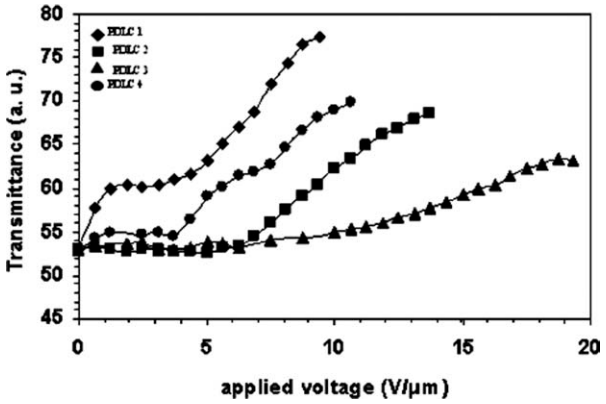

Figure 11 Transmitted intensity as function of the applied voltage for PDLCs 1–4 measured in *p*-polarization.

Figure 11. In all samples, the transmissivity increases with the field, which shows that the scattering losses are high at the beginning and reduce with applied electric field. The switching response of the PDLC samples is also shown in Figure 12. The switching voltage, rise time, and decay time of PDLCs 1–4 are presented in Table II. The rise time is defined as the time required for the transmittance to rise from 10 to 90% points of the waveform and the decay time is similarly defined as the time required for the transmittance to fall from 90 to 10% points of the waveform. Threshold (V_{10}) and operating (V_{90}) voltages of these films decrease along PDLC3 > PDLC2 > PDLC4 > PDLC1. The switching voltage depends on the morphology of the LC droplets and the electrical properties of the LC and the polymer matrix. Typically, the switching voltage is inversely proportional to the droplet size. Small droplets enhance the LC's elastic deformation energy, and thus larger voltages are required to reorient the LC molecules confined to the droplets and thus to switch on a PDLC. The enhanced elastic deformation energy associated with small droplets also leads to shorter turn off times. As presented in Table II, PDLC3, with smallest size of droplets, has the greatest switching voltage and shortest decay time as compared with the other three samples. However, UTMA based PDLC (PDLC1), with the greatest average size of LC droplets, has lowest amount of switching voltage and slowest rise and decay times. It is important to emphasize that there is a distribution of droplet sizes within typical PDLC films and the character of this distribution is related to the kinetics of the phase separation process.

CONCLUSION

In this work, we introduce a new multifunctional acrylate monomer; UTMA based PDLC. The synthesized UTMA is characterized by FTIR, ^{1}H-NMR, and ^{13}C-NMR spectroscopic techniques. The polymerization behaviors, LC phase separation, polymer/LC

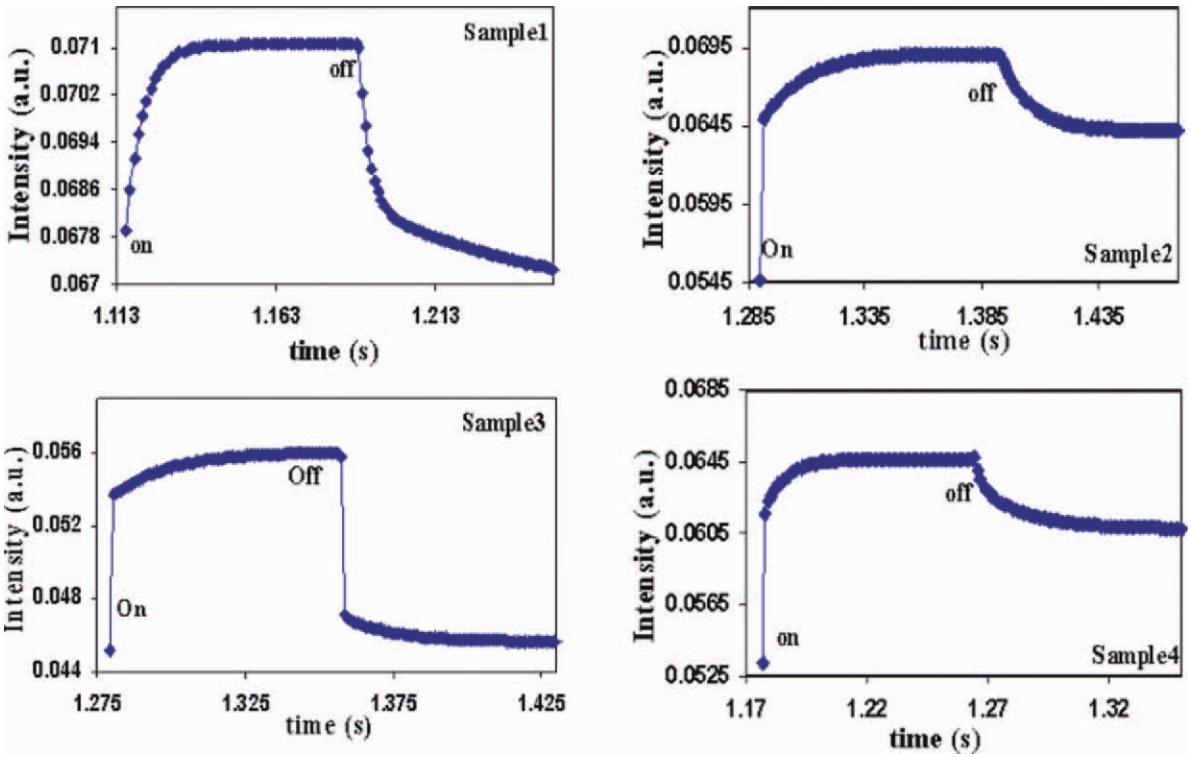

Figure 12 Dynamic measurement of transmittance for the switchable PDLCs corresponding to the on-off switching field 9.4, 13.7, 19.4, and 10.6 V/μm for PDLC1, PDLC2, PDLC3, and PDLC4, respectively. [Color figure can be viewed in the online issue, which is available at wileyonlinelibrary.com.]

morphology, and electro-optical performance of UTMA based PDLC is studied and compared with some well-known acrylate monomer compositions such as TMPTA and the combination of TMPTA and DPHPA. Interestingly, UTMA based PDLC shows considerably higher limiting conversion in comparison with other acrylate based PDLC samples. Using RTIR spectroscopy, it has been shown that this sample has also greater amount of polymerization rate, gel point bond conversion, and LC phase separation. In spite of the acrylate monomers, which show gel point conversions as low as 1.83–5.72%, UTMA reaches to its maximum rate at 19.5% conversion, which increases the participation of liquid-liquid demixing, and therefore increases the LC phase separation and droplet size. The UTMA also reduces the switching voltage significantly. However, due to the large droplet size, the response times were slightly slower than that of other samples. More investigation on UTMA and its combination with acrylate monomers for both PDLC and HPDLC applications is in progress. In future correspondences we will show that the HPDLC made by UTMA has up to 90% diffraction efficiency, which is promising as a good substitute to some common multifunctional monomers used in HPDLC.

References

1. Drzaic, P. Liquid Crystal Dispersion; World Scientific: Singapore, 1995.
2. Simoni, F. Non Linear Optical Properties of LC & PDLCs; World Scientific: Singapore, 1997.
3. Sutherland, R. L.; Natarajan, L. V.; Tondiglia, V. P.; Bunning, T. J. Chem Mater 1993, 5, 1533.
4. Fan, Y. H.; Lin, Y. H.; Ren, H.; Gauza, S.; Wu, S. T. Appl Phys Lett 2004, 84, 1233.
5. Nicoletta, F. P.; Chidichimo, G.; Cupelli, D.; Filpo, G. D.; Benedit-tis, M. D.; Gabriele, B.; Salerno, G.; Fazio, A. Adv Funct Mater 2005, 15, 995.
6. White, T. J.; Natarajan, L. V.; Bunning, T. J.; Tondiglia, V. P.; Guymon, C. A. Macromolecules 2007, 40, 1112.
7. LeGrange, J. D.; Carter, S. A.; Fuentes, M.; Boo, J.; Freeny, A. E.; Cleveland, W.; Miller, T. M. J. Appl Phys 1997, 81, 5984.
8. Kim, S. H.; Heo, C. P.; Park, K. S.; Kim, B. K. Polym Int 1998, 46, 143.
9. Ryu, J. H.; Choi, Y. H.; Suh, K. D. Colloids Surf A 2006, 275, 126.
10. Senyurt, A. F.; Warren, G.; Whitehead, J. B.; Hoyle, C. E. Polymer 2006, 47, 2741.
11. Leclercq, L.; Maschke, U.; Ewen, B.; Coqueret, X.; Mechernene, L.; Benmouna, M. Liq Cryst 1999, 26, 415.
12. Vaia, R. A.; Tomlin, D. W.; Schulte, M. D.; Bunning, T. J. Polymer 2001, 42, 1055.
13. Roussel, F.; Buisine, J. M.; Maschke, U.; Coqueret, X. Liq Cryst 1998, 24, 555.
14. White, T. J.; Liechty, W. B.; Natarajan, L. V.; Tondiglia, V. P.; Bunning, T. J.; Guymon, C. A. Polymer 2006, 47, 2289.
15. Odian, G. Principles of Polymerization, 4th ed.; Wiley: New York, 2004.
16. Natarajan, L. V.; Shepherd, C. K.; Brandelik, D. M.; Sutherland, R. L.; Chandra, S.; Tondiglia, V. P.; Tomlin, D.; Bunning, T. J. Chem Mater 2003, 15, 2477.
17. Carlsson, I.; Harden, A.; Lundmark, S.; Manea, A.; Rehnberg, N.; Svensson, L. In ACS Symposium Series 847; Belfield, K. D., Crivello, J. V., Eds.; American Chemical Society: Washington, DC, 2003.
18. Cotarca, L.; Eckert, H. Phosgenations-A Handbook; Wiley-VCH Verlag GmbH & Co. KGaA, Weinheim 122 2003.
19. Bhargava, R.; Wang, S. Q.; Koenig, J. L. Macromolecules 1999, 32, 8982.
20. Bhargava, R.; Wang, S. Q.; Koenig, J. L. Macromolecules 1999, 32, 8989.
21. Duran, H.; Meng, S.; Kim, N.; Hu, J.; Kyu, T.; Natarajan, L. V.; Tondigli, V.; Bunning, T. J. Polymer 2008, 49, 534.
22. Anseth, K. S.; Wang, C. M.; Bowman, C. N. Macromolecules 1994, 27, 650.
23. Mateo, J. L.; Calvo, M.; Bosch, P. J Polym Sci Part A: Polym Chem 2001, 40, 120.